6.UAP MEng Proposal: Fiber-coupled Ion Trap

Tony Hyun Kim

May 13, 2009

1 Basic info and personal statement

The project described in this proposal is my intended Course VI Master of Engineering thesis work with Prof. Isaac Chuang of the Quanta Group at the Center for Ultracold Atoms (CUA at RLE). I will begin work in the Fall 2009 semester, with a projected timeline consisting of three regular semesters, as well as Summer 2010.

My interest is in applied physics. In particular, I wish to explore and develop useful devices that go beyond those of standard microelectronics, which are based on the principle of current switching. This interest has led me to the field of quantum computation. Through this thesis work, I plan on gaining practical experience in device fabrication and laboratory optics, as well as deepening my theoretical understanding of quantum physics, especially in the context of AMO (atomic, molecular, optical) physics.

The organization of this document is as follows: first, I describe in non-technical terms the motivations and the objectives for the proposed fiber-coupled ion trap. Secondly, I give a theoretical discussion of the principles of the trap operation. In particular, I provide a list of routine atom-light manipulations, thereby highlighting the various ways in which the fiber-integrated trap can improve ion trapping as a platform for quantum computation. I then describe some of the progress that we have already made (in the Spring 2009 semester) towards the fiber trap. Finally, a projected timeline of the project is given.

2 Project introduction

We pursue planar ion traps as a platform for quantum computation. These structures can trap individual atomic ions, which are then used as qubits. The distinct advantage of planar traps is that they can be fabricated via standard silicon VLSI technology. This allows for arbitrary scaling of the devices, thus fulfilling one of the basic requirements for implementing quantum information algorithms and quantum simulations.

The manipulation of the atomic ion qubit, as well as its state readout, is achieved by atom-light interactions. However, at the moment, the coupling of the atomic qubit with the external laser remains problematic, as the laser must be aligned frequently and carefully with respect to the trap. In other words, despite the scalability of planar ion traps on a chip, the system to interface to those qubits is extremely cumbersome to maintain. This effectively prevents large-scale planar ion devices, since it is unfeasible to address many ions at a given time.

Hence, in this project, we propose to fabricate a planar ion trap on the surface end of an optical fiber. The general structure is illustrated in Figure 1.

The advantages of such a structure is that, by design, the ion is held at a precise position with respect to the light source, thereby removing the difficult alignment efforts in interfacing to the atomic qubit. Furthermore, by placing a mirror above the fiber, the trapped ion can be effectively placed in an optical cavity, thereby increasing

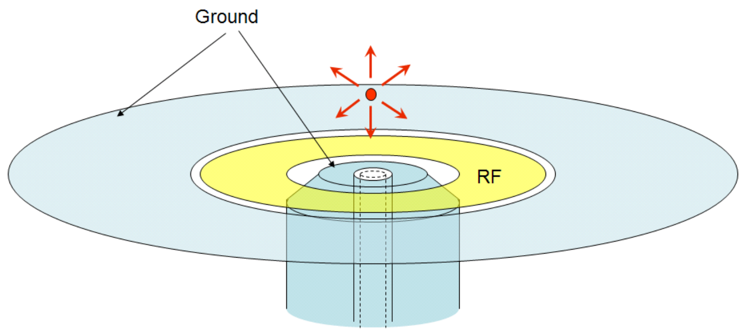

Figure 1: Schematic of the fiber-coupled ion trap. The red dot represents the trapped ion interacting with the light from the fiber below. The annular electrodes are utilized to trap the ion above the fiber.

the efficiency of atom-light coupling.

The objective of the project is to experimentally produce such a fiber ion trap, and to verify its performance with the ^{88}Sr^{+} ion. Successful completion of this project will yield a convenient primitive in the integrated optical approach to quantum computation.

3 Principles of operation for the ^{88}Sr^{+} ion-trap

We now summarize the principles of operation behind the ion trap presented in Figure 1, whose electrode geometry is referred to as the "planar point trap" (a.k.a. "point Paul trap"). For the mathematical details, the reader is referred to Ghosh[1]. The discussion here is heavily based on the thesis of Christopher E. Pearson[2] who completed a theoretical analysis of the planar point trap.

3.1 Ion Trapping

3.1.1 Electric potential

Consider the following idealization of the planar point trap: there is no space between the RF and ground electrodes, and the outer ground plane extends to infinity. This approximation is illustrated in Figure 2. We use cylindrical coordinates (z, r) aligned with the axis of the point trap. (In particular, $z = 0$ is the plane of the trap.)

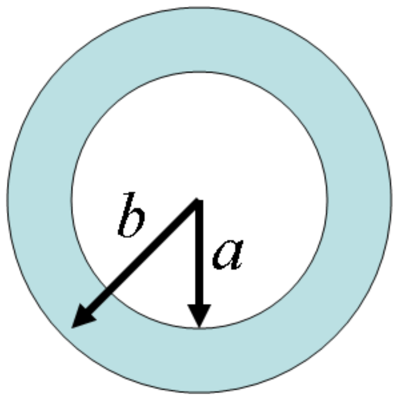

Figure 2: A top down view of the idealized planar point trap. The electrode configuration presented here is also that of the proposed fiber-coupled trap. The blue electrode (an annulus with inner radius a and outer radius b) is at a potential V_{RF}. The white regions (inside and outside of the annulus) represent potential ground.

In practice, the annular electrode carries a time-varying potential. For the analysis, however, we solve the static problem at a particular instant in time using separation of variables. A multiplicative sinusoidal time dependence is then assumed for the final result. This approach is justified as long as the "characteristic velocity" (say, the trap size divided by the period of the RF drive) is much smaller than the electromagnetic field propagation velocity, c.

Suppose the RF electrode is at a potential V_{RF} at a particular instant. The results of [2] are summarized here. The instantaneous potential anywhere above the trap ($z > 0$) is given by:

$$\phi(z,r) = V_{RF} \cdot \phi_0(z,r) \tag{1}$$

$$\phi_0(z,r) = \int_0^\infty \left[bJ_1(kb) + dJ_1(kd)\right] e^{-kz} J_0(kr)dk \tag{2}$$

where $d = b - a$ is the width of the annular (RF) electrode, and J_n are the Bessel functions of the first kind of order n.

The on-axis ($r = 0$) potential can be analytically computed, and is shown in Eq. 3. This gives a benchmark for evaluating the validity of the three-dimensional, numerical solution.

$$\phi(z, r = 0) = V_{RF} \left[\frac{1}{\sqrt{1 + d^2/z^2}} - \frac{1}{\sqrt{1 + b^2/z^2}} \right] \tag{3}$$

Finally, the cosine dependence of the RF potential $V_{RF}(t) = V_{RF}\cos(\Omega t)$ is reflected in the final result as a multiplicative time modulation:

$$\phi(\vec{r}, t) = V_{RF} \cdot \phi_0(\vec{r}) \cos(\Omega t) \tag{4}$$

3.1.2 Pseudopotential

The motion of a charged particle in a sinusoidal time-dependent potential of the type Eq. 4 can be divided into a low-frequency *secular* motion, and a high-frequency *micromotion*[1]. (The micromotion frequencies are sidebands of the drive frequency Ω.) Because the latter is generally of smaller amplitude, the operation of the trap can be adequately analyzed by focusing on the secular motion.

The analysis of the secular trajectory is further simplified by the introduction of a quantity known as the *pseudopotential*, Ψ. The pseudopotential represents the time-averaged potential experienced by the particle, and is defined by:

$$\Psi(\vec{r}) = \frac{QV_{RF}^2}{4m\Omega^2} \left|\nabla\phi_0(\vec{r})\right|^2 \tag{5}$$

where Q, m are the charge and mass of the target particle, respectively. The secular motion of the particle in a time-dependent potential (Eq. 4) is equal to the motion of the same particle in the time-independent pseudopotential (Eq. 5).

In the planar point trap, the pseudopotential is given by:

$$\Psi(z,r) = \frac{QV_{RF}^2}{4m\Omega^2}\left[\left|\frac{d\phi_0}{dz}\right|^2 + \left|\frac{d\phi_0}{dr}\right|^2\right] \tag{6}$$

$$\frac{d\phi_0}{dz} = \int_0^\infty -k\left[bJ_1(kb) - dJ_1(kd)\right] e^{-kz} J_0(kr) dk \tag{7}$$

$$\frac{d\phi_0}{dr} = \int_0^\infty -k\left[bJ_1(kb) - dJ_1(kd)\right] e^{-kz} J_1(kr) dk \tag{8}$$

which is numerically evaluated in the upcoming section using typical dimensions of the fiber-coupled trap. If the pseudopotential in Eq. 6 has confining characteristics, then we have a structure which will trap the charged particle.

3.1.3 Numerical example for fiber trap dimensions

Let $a = 0.125$ mm, and $b = 1.075$ mm. These dimensions correspond to the schematic of the "Yodok delta" fiber-coupled trap shown in Fig. 5.

The pseudopotential is computed by numerically evaluating Eqs. 6, 7 and 8. The validity of the numerical procedure has been established by comparing the numerical on-axis $\frac{d\phi_0}{dz}$ against the derivative of the analytic solution, Eq. 3.

The pseudopotential as a function of (z, r) is shown in Figure 3. We plot the logarithm of $\Psi_0 = \left|\frac{d\phi_0}{dz}\right|^2 + \left|\frac{d\phi_0}{dr}\right|^2$. This quantity was laboriously calculated using my classical Intel computer.

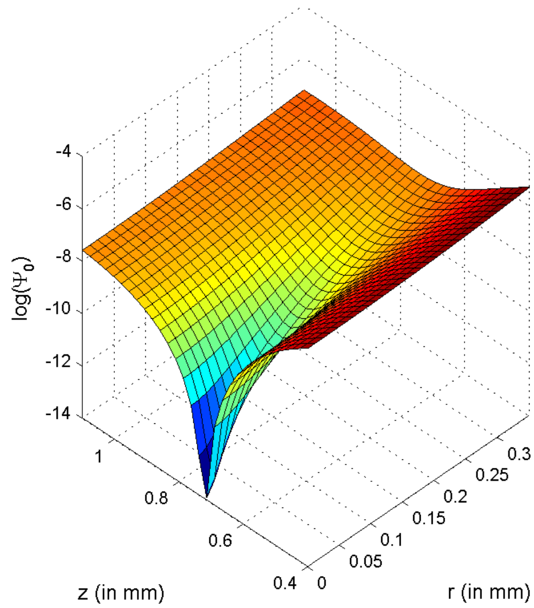

Figure 3: The 3D pseudopotential for $a = 0.125$ mm and $b = 1.075$ mm. Based on the stable minimum near $z = 0.7$ mm, the trap is confining.

According to our idealized model, it is clear that the secular motion is confined at roughly $z = 0.7$ mm above the trap.

3.2 $^{88}Sr^{+}$ Level Structure

We have shown that a charged particle can be trapped by the electrodes of the fiber-coupled trap. Recall that the main objective of fiber integration is to facilitate the manipulation of the ion by laser light. Hence, we now summarize the relevant level structure of the $^{88}Sr^{+}$ ion, and the ways in which that structure is used for our purposes. The information in this section has been extracted from various past Quanta theses, for instance, [3] and [4].

The $^{88}Sr^{+}$ ion has been chosen since it posesses a single valence electron, and because all of the relevant electronic transitions can be achieved with diode lasers. Figure 4 illustrates the relevant $^{88}Sr^{+}$ electronic level structure.

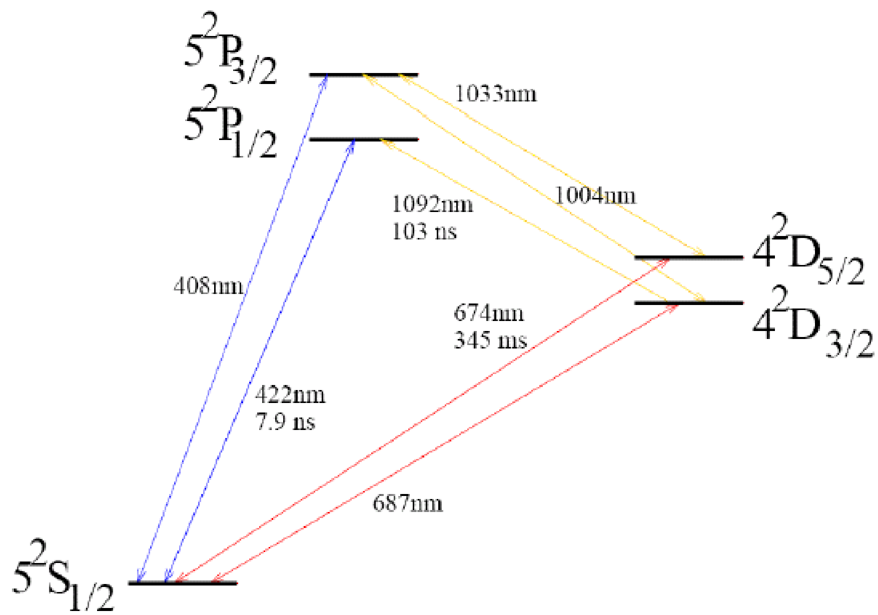

Figure 4: Level structure showing the relevant electronic states of the $^{88}Sr^+$ ion. The array of available electronic levels, and the convenience of diode lasers to provide the transition wavelengths (422, 674, 1033 and 1092 nm lasers are already employed in the lab[3]) make this ion a versatile system for quantum computation.

Below, we list some of the routine laser manipulations.

- **^{88}Sr$^+$ as a qubit using the states $5S_{1/2}$ and $4D_{5/2}$.** The 345 ms lifetime of this 674 nm transition sets a high upper-limit on the duration of coherent control.

- **State detection using the $5S_{1/2} \to 5P_{1/2}$ transition.** The rapid decay of the 422 nm transition can be exploited for state detection. Specifically, the scattering of 422 nm beam is a signature of the $5S_{1/2}$ state. (As opposed to, say, the $4D_{5/2}$ state.)

- **Doppler cooling.** The same $5S_{1/2} \to 5P_{1/2}$ transition can be used for slowing the ion, by the use of a 422 nm laser counterpropagating against the direction of ion motion. (Simultaneously, we use the 1092 nm laser to prevent shelving into the dark state $4D_{3/2}$.)

- **Sideband cooling.** The ion is cooled to the motional ground state of the trap by using a 674 nm laser ($5S_{1/2} \rightarrow 4D_{5/2}$) red-detuned by the energy of one motional quanta of the trap. The $4D_{5/2}$ state is then pumped to the $5P_{3/2}$ state in order to allow the ion to spontaneously emit to the $5S_{1/2}$ state at a reasonable rate, thereby completing the sideband-cooling cycle: $5S_{1/2} \rightarrow 4D_{5/2} \rightarrow 5P_{3/2} \rightarrow 5S_{1/2}$.

As can be seen, optical control of the atomic ion is crucial at every stage of the experiment: ion preparation, coherent manipulation, and state readout. Therefore, our fiber-integrated ion trap will significantly improve the usability of the ion trap for quantum computation purposes.

4 Spring 2009 Fabrication Efforts

One of the challenges in constructing the fiber-trap is to efficiently utilize fabrication equipment, which are generally designed to work with wafers. So, we must come up with a strategy for patterning three annular electrodes (recall Figure 1) on a small, non-traditional structure, i.e. the end of a fiber.

Based on the work that Yufei Ge and I have already completed in Spring 2009, we believe that a complete fabrication of the fiber trap is definitely possible.

4.1 General design

Our current fabrication strategy is based on the "Yodok Delta" design by Dr. Tae-Hyun Kim. The Yodok Delta schematic is shown in Figure 5.

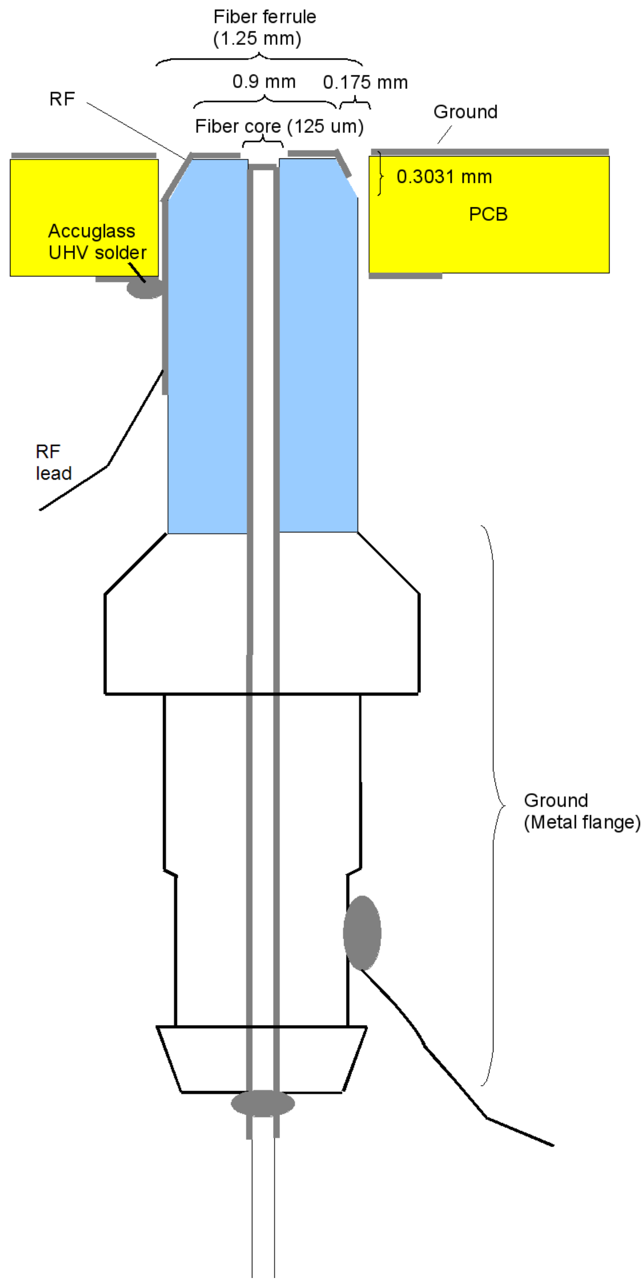

Figure 5: The "Yodok Delta" schematic for the fiber-coupled ion trap. Note that the PCB (which has the ground plane), the ferrule (RF electrode) and fiber (ground electrode) are all separable parts. This allows the fabrication to be completed piecewise.

The important feature is that the three annular regions are defined on three separate parts of the assembly; and are only brought together at the final construction. This is convenient in that it allows the fabrication to be completed piecewise.

4.2 Fabrication details

4.2.1 Optical fiber

We must make a ground plane on the surface of the fiber, but with a cutaway over the fiber core, so that the fiber light can be transmitted. A cartoon depiction of the process flow is shown in Figure 6.

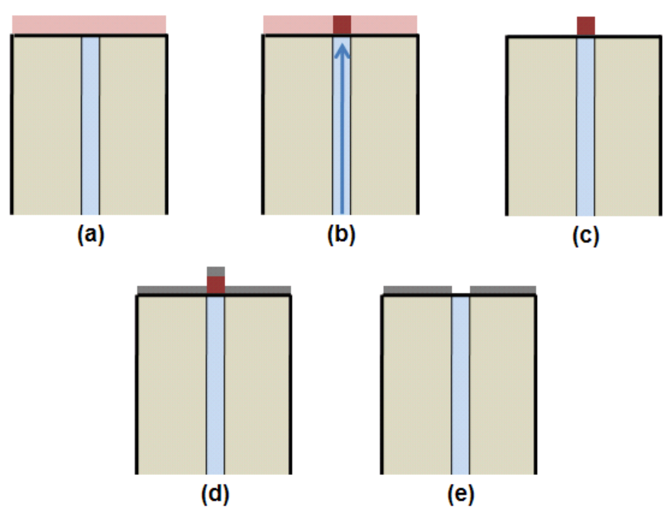

Figure 6: Fiber process flow. Steps (a), (b) and (c) show the patterning of the photoresist. Note, in panel (b), that the light is delivered from the fiber itself. Step (d) shows the result of silver deposition. Step (e) shows final liftoff.

1. The fiber is prepared by stripping away the outermost cladding. This allows the fiber to be inserted into the ferrule later, without further stripping.

2. We coat and pattern the surface of the fiber with positive photoresist. At the

end, only the fiber core should be covered by the resist. We use NR9-3000 as the photoresist. The fiber is coated by the following procedure:

(a) Coat a dummy wafer with $2 - 3$ μm-thick NR9-3000 by spinning at 4000 rpm. Prebake the wafer at 150°C for at least 1 minute.

(b) Dip the fiber into the NR9-3000-covered dummy wafer.

(c) Pre-bake the fiber tip for 1 minute at 200°C. We achieve this by touching the side of the hot plate with the fiber.

(d) The photoresist is exposed *through the fiber*. Prior to fabrication, the other (uncoated) end of the fiber is fitted with a fiber coupling package, and is configured for 405 nm light.

(e) Resist is developed in RD6. The developing time is highly variable, depending on the original dip into the photoresist film. We have used approximately 20 seconds.

3. Deposit 7.5 nm of titanium as an adhesion layer. Deposition of 300 nm of silver by evaporation.

4. Liftoff with acetone.

Figure 7 is a photo of the fiber tip, with the core covered by photoresist.

4.2.2 Ferrule

The ferrule contains the RF electrode. The main challenge is to make sure that this electrode does not short with the ground plane on the PCB or on the fiber. The latter requirement is the greater difficulty. We also need to be able to make electrical contact from the RF source. Clearly, we have to make the RF connection from below

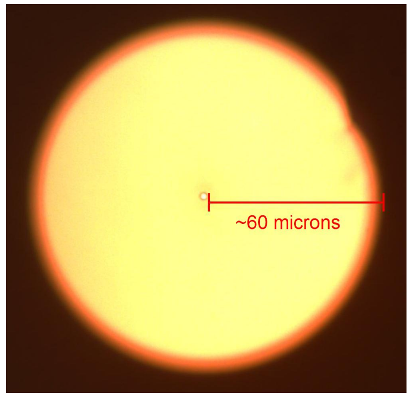

Figure 7: Photograph of the fiber tip. The fiber core is covered by photoresist.

the PCB plane, since otherwise the trapping region will be severely perturbed by the connector lead.

1. Begin by plating the ferrule tip with 500 nm-thick aluminum. (Again, 7.5 nm of Ti is used for adhesion.) We purposely coat the side of the ferrule tip as well, in order to gain electrical access to the electrode from below the PCB plane.

2. Etch away metal from the center of the ferrule, in order to prevent shorts between the fiber and ferrule electrodes. The process is detailed below, and a cartoon process flow is illustrated in Figure 8.

   (a) The ferrule tip is dipped in photoresist.

   (b) Aluminum etchant, NH_4OH:H_2O_2:H_2O::1:1:4, is introduced into the barrel of the ferrule via a syringe. We wait a minute or so for the etching.

   (c) Remove photoresist with acetone.

Figure 9 is a photograph of the ferrule tip following the above fab process. The aluminum has been etched from the center for approximately 20 seconds.

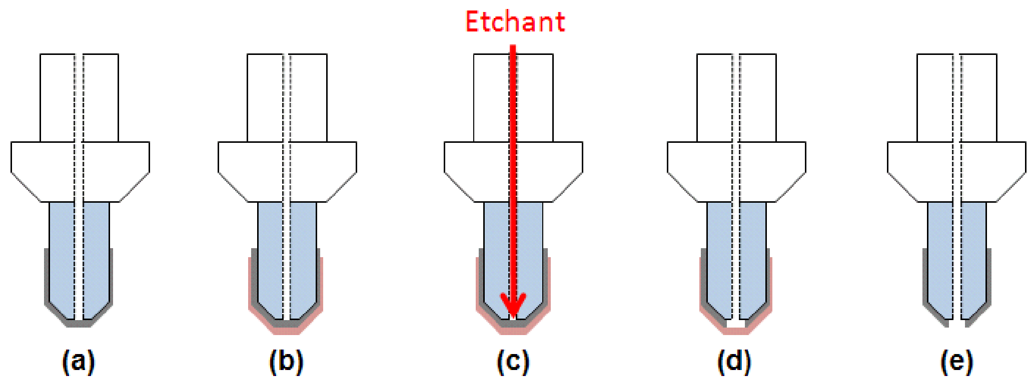

Figure 8: Ferrule process flow. (a) Basic ferrule whose tip has been coated with aluminum. (b) The tip is coated with photoresist. (c) Etchant is introduced through the fiber barrel. (d) Aluminum is etched from the center. (e) Photoresist is removed.

4.2.3 PCB

The PCB contains only a very large ground plane, and bias plates (not shown in Fig. 5 schematic). Hence, its manufacture is trivial. The desired PCB could even be fabricated at a standard PCB shop.

4.3 Foreseeable difficulties

- At the final assembly, the patterned fiber must be inserted into the ferrule. However, especially with the added thickness, the insertion may be difficult, and may damage our fabricated structure on the fiber. Therefore, we may have to fabricate the fiber after it has been inserted into the ferrule.

- The ultimate objective of planar ion trap quantum computing is scalability. On the other hand, the fabrication method described here is very manual. At this early stage, the immediate goal is to fabricate one working fiber-coupled trap. In the future, however, the fab procedure must be drastically modified in order to take advantage of VLSI scalability.

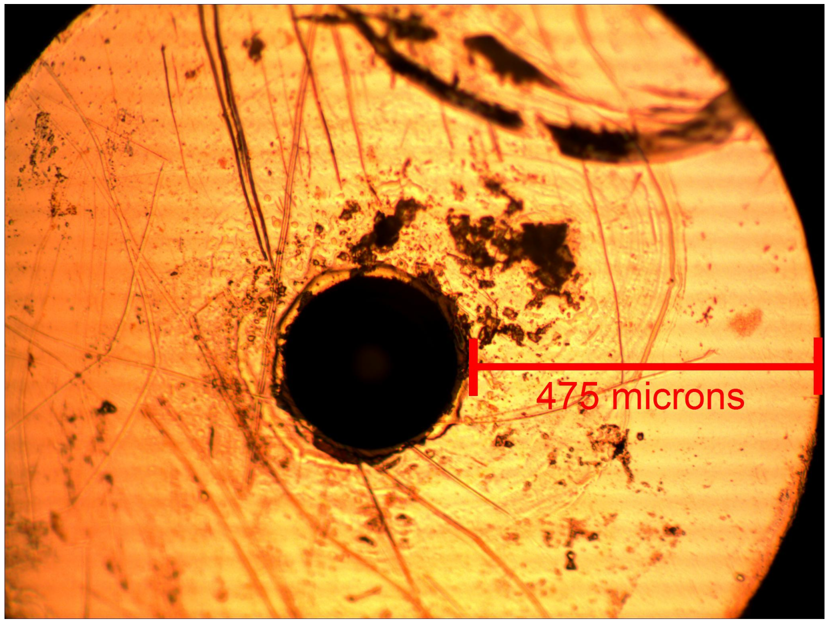

Figure 9: Photograph of the ferrule following the fab procedure. The ferrule tip has been plated with aluminum. Note that the aluminum has been etched away from the center of the ferrule.

5 Proposed Plan

We now detail the experimental objectives of the project, in chronological order.

5.1 Fabrication of the fiber-ion trap.

We have already made progress on this sub-goal. However, we have yet to combine the three parts (fiber, ferrule and PCB) together. Some of the open questions that still remain are:

- How to mount the assembly so that it is mechanically sound.
- Whether it is possible to insert the fiber (with its added thickness) into the ferrule without damaging its electrode and the face of the fiber core.

In particular, the completed structure must pass the following criteria:

- Electrical isolation between the three electrodes.
- The RF electrode must be able to carry hundreds of volts without arcing.
- Light should be coupled through the fiber, and its output mode should be examined. We are looking for defects in the face of the fiber core.

I expect to finish a first complete assembly of the trap by October 2009 at the latest.

5.2 Verification of the trapping capabilities of the fiber trap, without using the integrated fiber (i.e. verification as a conventional planar trap).

We expect to approach this objective in two directions. The two approaches can be taken simultaneously.

First, we plan on fabricating planar point traps on a regular wafer. We are interested in this because point traps that have dimensions of the proposed fiber trap have not yet been demonstrated in the Quanta group. The existing experimental apparatus does not need to be modified for this approach. Furthermore, it is easy to fabricate many point traps with slightly differing dimensions, to experimentally search for the optimal parameters.

Secondly, we would utilize the completed fiber trap itself to trap an ion. Only the trapping capabilities will be investigated; that is, the fiber is not used to perform any ion manipulations.

This step will be completed by December 2009.

5.3 Deployment of the integrated fiber.

5.3.1 Theoretical

From a simple numerical simulation (Section 3.1.3), we have estimated the vertical height of the ion above the trap. From the experimental test of the fiber trap, we can also measure this height.

Given this distance, along with the fiber dimensions and the strength of whatever transition that we wish to drive, one can calculate the power requirements for ion manipulation.

When the fiber is utilized for light collection, then the collection efficiency corresponding to the geometry can similarly be investigated.

5.3.2 Experimental

This step requires modifications to the experimental chamber, in order to pass the fiber into the vacuum chamber.

We would begin by using fiber-delivered light to do state detection of the $5S_{1/2}$ state. We deliver the 422 nm beam using the fiber, but collect the scattered light through standard means. This is the simplest "sanity-check" procedure for establishing the correct operation of the fiber.

The next step is to sideband-cool the ion. Thorlabs sells multimode fibers that have $> 99\%$ transmission of the frequency range of interest (400 - 1100 nm)[5].

On the other hand, Doppler cooling is more complicated, since the ion source has to be situated in such a way that the fiber-coupled beam is counterpropagating to its direction of approach (when coming towards the trap).

Also, state detection where the fiber is used for light collection may be more difficult, since efficient light collection depends on factors such as numerical aperture which we have not explicitly optimized in the construction of the fiber trap.

Therefore, the last two criteria may only be met by several iterations of trap design. I expect to accomplish state-detection (delivery) and possibly sideband-cooling within the first few months of the Spring 2010 term (March 2010 or so); however, the latter objectives may take up to the end of Summer 2010.

5.4 MEMS Mirror

The interaction of the light with the ion can be enhanced by constructing a mirror to place the ion in a cavity. This is a longer-term goal, that would start at the earliest in the Fall 2010 semester. The procedure in which the mirror is mounted across from the fiber output face is currently an open question.

In any case, the experimental signature of this objective would be, for example, a more efficient scattering of light in the state detection of $5S_{1/2}$ (again, where the fiber is used to deliver the light).

5.5 Ion source ("oven")

The integration of the ion source into the fab process would be an improvement over the current diffusion-based loading. The particular layout would be influenced by whether we are attempting to Doppler-cool through the fiber. Again, this is a longer-term objective, that would also start at the earliest in Fall 2010.

5.6 Miscellaneous

I plan on begin writing the thesis in the Fall 2010 Semester. Before this time, the fabrication process for the fiber-trap should be optimized as to take advantage of VLSI fab methods.

References

[1] Ghosh, Pradip K. *Ion Traps.* Oxford Science Publications, 1995.

[2] Pearson, Christopher Elliott. *Theory and Application of Planar Ion Traps.* Massachusetts Institute of Technology, MS Thesis 2006.

[3] George, Elizabeth Marie. *Fiber Optic Integration in Planar Ion Traps.* Massachusetts Institute of Technology, BS Thesis 2008.

[4] Shewmon, Ruth. *Coherent Manipulation of Trapped* $^{88}Sr^{+}$ *using the* $4D_{5/2} \rightarrow 5S_{1/2}$ *transition* Massachusetts Institute of Technology, BS Thesis 2008.

[5] Thorlabs, Inc. 0.48 *NA Hard Polyer Clad Multimode Fiber.* http://www.thorlabs.com/Thorcat/12200/12247-S01.pdf